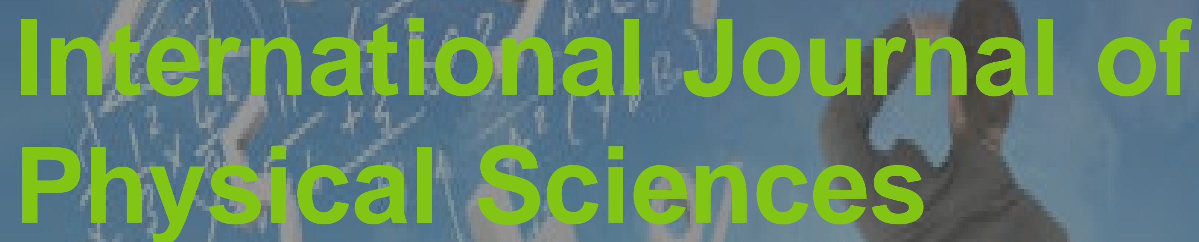

International Journal of Physical Sciences

Volume 9 Number 12 30 June, 2014
ISSN 1992-1950

ABOUT IJPS

The **International Journal of Physical Sciences (IJPS)** is published weekly (one volume per year) by Academic Journals.

International Journal of Physical Sciences (IJPS) is an open access journal that publishes high-quality solicited and unsolicited articles, in English, in all Physics and chemistry including artificial intelligence, neural processing, nuclear and particle physics, geophysics, physics in medicine and biology, plasma physics, semiconductor science and technology, wireless and optical communications, materials science, energy and fuels, environmental science and technology, combinatorial chemistry, natural products, molecular therapeutics, geochemistry, cement and concrete research, metallurgy, crystallography and computer-aided materials design. All articles published in IJPS are peer-reviewed.

Contact Us

Editorial Office: ijps@academicjournals.org

Help Desk: helpdesk@academicjournals.org

Website: http://www.academicjournals.org/journal/IJPS

Submit manuscript online http://ms.academicjournals.me/

Editors

Prof. Sanjay Misra
Department of Computer Engineering, School of Information and Communication Technology Federal University of Technology, Minna, Nigeria.

Prof. Songjun Li
School of Materials Science and Engineering, Jiangsu University, Zhenjiang, China

Dr. G. Suresh Kumar
Senior Scientist and Head Biophysical Chemistry Division Indian Institute of Chemical Biology (IICB)(CSIR, Govt. of India), Kolkata 700 032, INDIA.

Dr. 'Remi Adewumi Oluyinka
Senior Lecturer, School of Computer Science Westville Campus University of KwaZulu-Natal Private Bag X54001 Durban 4000 South Africa.

Prof. Hyo Choi
Graduate School Gangneung-Wonju National University Gangneung, Gangwondo 210-702, Korea

Prof. Kui Yu Zhang
Laboratoire de Microscopies et d'Etude de Nanostructures (LMEN) Département de Physique, Université de Reims, B.P. 1039. 51687, Reims cedex, France.

Prof. R. Vittal
Research Professor, Department of Chemistry and Molecular Engineering Korea University, Seoul 136-701, Korea.

Prof Mohamed Bououdina
Director of the Nanotechnology Centre University of Bahrain PO Box 32038, Kingdom of Bahrain

Prof. Geoffrey Mitchell
School of Mathematics, Meteorology and Physics Centre for Advanced Microscopy University of Reading Whiteknights, Reading RG6 6AF United Kingdom.

Prof. Xiao-Li Yang
School of Civil Engineering, Central South University, Hunan 410075, China

Dr. Sushil Kumar
Geophysics Group, Wadia Institute of Himalayan Geology, P.B. No. 74 Dehra Dun - 248001(UC) India.

Prof. Suleyman KORKUT
Duzce University Faculty of Forestry Department of Forest Industrial Engineeering Beciyorukler Campus 81620 Duzce-Turkey

Prof. Nazmul Islam
Department of Basic Sciences & Humanities/Chemistry, Techno Global-Balurghat, Mangalpur, Near District Jail P.O: Beltalapark, P.S: Balurghat, Dist.: South Dinajpur, Pin: 733103,India.

Prof. Dr. Ismail Musirin
Centre for Electrical Power Engineering Studies (CEPES), Faculty of Electrical Engineering, Universiti Teknologi Mara, 40450 Shah Alam, Selangor, Malaysia

Prof. Mohamed A. Amr
Nuclear Physic Department, Atomic Energy Authority Cairo 13759, Egypt.

Dr. Armin Shams
Artificial Intelligence Group, Computer Science Department, The University of Manchester.

Editorial Board

Prof. Salah M. El-Sayed
Mathematics. Department of Scientific Computing.
Faculty of Computers and Informatics,
Benha University. Benha ,
Egypt.

Dr. Rowdra Ghatak
Associate Professor
Electronics and Communication Engineering Dept.,
National Institute of Technology Durgapur
Durgapur West Bengal

Prof. Fong-Gong Wu
College of Planning and Design, National Cheng Kung University
Taiwan

Dr. Abha Mishra.
Senior Research Specialist & Affiliated Faculty.
Thailand

Dr. Madad Khan
Head
Department of Mathematics
COMSATS University of Science and Technology
Abbottabad, Pakistan

Prof. Yuan-Shyi Peter Chiu
Department of Industrial Engineering & Management
Chaoyang University of Technology
Taichung, Taiwan

Dr. M. R. Pahlavani,
Head, Department of Nuclear physics,
Mazandaran University,
Babolsar-Iran

Dr. Subir Das,
Department of Applied Mathematics,
Institute of Technology, Banaras Hindu University,
Varanasi

Dr. Anna Oleksy
Department of Chemistry
University of Gothenburg
Gothenburg,
Sweden

Prof. Gin-Rong Liu,
Center for Space and Remote Sensing Research
National Central University, Chung-Li,
Taiwan 32001

Prof. Mohammed H. T. Qari
Department of Structural geology and remote sensing
Faculty of Earth Sciences
King Abdulaziz UniversityJeddah,
Saudi Arabia

Dr. Jyhwen Wang,
Department of Engineering Technology and Industrial Distribution
Department of Mechanical Engineering
Texas A&M University
College Station,

Prof. N. V. Sastry
Department of Chemistry
Sardar Patel University
Vallabh Vidyanagar
Gujarat, India

Dr. Edilson Ferneda
Graduate Program on Knowledge Management and IT,
Catholic University of Brasilia,
Brazil

Dr. F. H. Chang
Department of Leisure, Recreation and Tourism Management,
Tzu Hui Institute of Technology, Pingtung 926,
Taiwan (R.O.C.)

Prof. Annapurna P.Patil,
Department of Computer Science and Engineering,
M.S. Ramaiah Institute of Technology, Bangalore-54,
India.

Dr. Ricardo Martinho
Department of Informatics Engineering, School of Technology and Management, Polytechnic Institute of Leiria, Rua General Norton de Matos, Apartado 4133, 2411-901 Leiria,
Portugal.

Dr Driss Miloud
University of mascara / Algeria
Laboratory of Sciences and Technology of Water
Faculty of Sciences and the Technology
Department of Science and Technology
Algeria

International Journal of Physical Sciences

Table of Contents: Volume 9 Number 12, 30 June, 2014

ARTICLES

Measurement and modeling of the effect of gamma irradiation on radiofrequency dielectric properties of bovine kidney tissue 275
E. H. Agba, T .Sombo and T.A Ige

Research in physical properties of AlxGa1-xAs III-V Arsenide ternary semiconductor alloys 281
Alla Srivani, Vedam Ram Murthy and G. Veera Raghavaiah

academicJournals

Vol. 9(12), pp. 275-280, 30 June, 2014
DOI: 10.5897/IJPS12.314
ISSN 1992 - 1950
Article Number: 28AC6A245856
Copyright © 2014
Author(s) retain the copyright of this article
http://www.academicjournals.org/IJPS

International Journal of Physical Sciences

Full Length Research Paper

Measurement and modeling of the effect of gamma irradiation on radiofrequency dielectric properties of bovine kidney tissue

E. H. Agba[1]*, T .Sombo[2] and T.A Ige[3]

[1]Department of Physics, Benue State University, P. M. B. 102119 Makurdi, Benue State, Nigeria.
[2]Department of Physics, University of Agriculture, P. M. B. 2373, Makurdi, Benue State. Nigeria.
[3]Department of Physics, National Hospital Abuja, Nigeria.

Received 15 April 2012; Accepted 21 June, 2013

The effect of gamma irradiation on the radiofrequency dielectric properties of bovine kidney tissue has been investigated using gamma irradiator (Gs 1000), booton (7200) capacitance meter, signal generator (Lodstars SG-416013) and Dielectric cells Mathematic models of the following dielectric structural parameter, Dielectric spread parameter (α), dielectric decrement (Δ) and Dielectric relaxation time (τ), were also developed. The mathematics models were found to be polynomial functions of degree 4,4, and 5 respectively. The coefficient of fit for dielectric decrement, relaxation time and spread parameter (α), were found to be 98.2, 83.9 and 99.5, respectively. This shows that, the mathematical model can be effectively used to generate dielectric data that will facilitate the prediction of the extent of mammalian kidney tissue damage in gamma irradiation doses regime usually encountered in diagnostic and therapeutic radiology.

Key word: Gamma irradiation, spread parameter (α), dielectric decrement (Δ), dielectric relaxation time (τ), dielectric permittivity (ε').

INTRODUCTION

The dielectric methods of investigating structural and molecular characteristics of biological tissues is a well established techniques (Essex et al., 1975; Kyber et al., 1991; and Laogun et al., 2005). They have been frequently used to study changes in material composition, cell structure and water content under certain physical conditions (Laogun, 1986). The common feature of all these methods is that, the biological sample is contained in a sample holder and its complex permittivity is measured at various discrete frequency points (Burdette et al., 1980; Grant et al., 1978). Alterations or change induced to biological tissues is as a result of the its interaction with ionizing radiation can be measured or inferred from βeta-dielectric dispersion properties of the irradiated tissues. These studies are prompted by the pride of place given to the use of ionizing radiation in diagnostic and therapeutic applications in healthcare and the need to established safety radiation levels (Laogun et al., 2005; and Agba et al., 2008).

Mathematical models of biological tissues provides

*Corresponding author. E-mail: msendoom@yahoo.com
Author(s) agree that this article remain permanently open access under the terms of the Creative Commons Attribution License 4.0 International License

Table 1. The mean a.c conductivity of ϒ-irradiated and non-irradiated bovine kidney from frequency range 0.5 to 50.0 MHz.

	Conductivity (σ)								
Frequency (MHZ) / Dose (Gy)	0.5	1.0	2.0	5.0	10	20	30	40	50
0	212.1 ± 34.2	219.0 ± 29.6	220.8 ± 40.2	262.9 ± 20.1	357.5 ± 56.6	432.6 ± 12.5	529.1 ± 18.6	652.1 ± 14.7	673.1 ± 28.9
1	259.4 ± 21.3	274.4 ± 18.6	274.4 ± 11.6	297.2 ± 23.0	402.1 ± 21.2	498.9 ± 25.5	566.8 ± 44.1	672.6 ± 68.2	682.8 ± 56.2
4	355.9 ± 30.2	359.8 ± 24.6	369.5 ± 37.8	370.3 ± 44.2	468.3 ± 25.3	587.7 ± 55.4	613.5 ± 40.7	695.0 ± 33.3	735.7 ± 21.1
11	366.3 ± 41.8	375.2 ± 64.2	395.3 ± 48.2	396.1 ± 76.4	466.3 ± 34.3	662.6 ± 42.1	675.7 ± 29.8	732.7 ± 45.6	746.3 ± 40.0
20	482.0 ± 16.3	505.1 ± 49.8	521.4 ± 53.0	531.9 ± 51.5	569.9 ± 34.8	675.7 ± 37.3	680.3 ± 47.2	746.7 ± 18.8	766.6 ± 46.2
43	519.5 ± 58.2	519.5 ± 41.6	537.6 ± 33.7	578.1 ± 46.3	579.7 ± 11.3	678.0 ± 38.2	712.0 ± 49.3	746.7 ± 41.5	781.5 ± 23.4
60	584.8 ± 60.1	598.9 ± 46.4	600.8 ± 21.8	602.6 ± 44.5	647.3 ± 29.4	690.0 ± 63.1	709.3 ± 28.4	746.9 ± 19.6	785.8 ± 13.4
85	614.1 ± 21.8	630.9 ± 29.7	658.9 ± 40.3	685.0 ± 53.0	699.3 ± 29.3	717.1 ± 38.7	746.9 ± 74.2	759.2 ± 53.4	794.9 ± 36.4

reasonable mathematical approximation of the physco-chemical changes occurring in a biological systems and is calibrated against real data obtained from experimental investigations. Effect of Ionizing radiations on human health has been reported by researchers such as Pethig (1991), AAMP (1992), UNSCEAR (1993), Roger (2006) and Russel and Bradley (2007). This study is aimed at modeling the effect of gamma irradiation on Bovine tissue at radiofrequency so as to predict its effects on mammalian tissues at doses within the diagnostic and therapeutic dose regime often encountered in radiology.

METHODOLOGY

The kidney tissue samples were excised from certified freshly slaughtered adult cow at Gwagwalada Central Abattoir in Gwagwalada Area Council Abuja, Nigeria. The excised tissue samples were washed with double distilled water and preserved in laboratory oven maintained at a temperature of 37± 0.5°C for 6 h so as to remove water from its surface. The samples were sealed and labeled in eight (8) plastic film bags. They were irradiated while the sample holders were positioned along their length at the centre of the irradiation field with irradiation doses: 0 Gy, 1 Gy, 4 Gy,11 Gy, 20 Gy,43 Gy, 60 Gy and 85 Gy, respectively.

The sample cells used in this research were constructed and calibrated in line with the method of Laogun et al. (2005) and Agba et al. (2008). The gamma irradiator (GS 1000) located at the Gamma irradiation facility (GIF) unit of National Nuclear Technology Centre, Abuja was used for the irradiation of the bovine kidney tissue samples at the dose rate of 0.36 kGy/h. Dielectric measurements were carried out using boonton (7200) capacitance meter in conjuction with signal generators (Lodstar, SG-416013 and Harris, G857993). The effective capacitance ΔC and dissipation factor (tanδ) of the gamma irradiated kidey tissue samples were first measured after which the dielectric permittivity (ε'') and dielectric conductivity (σ) were obtained using the equations below:

$$\Delta C = k\varepsilon' \quad (1)$$

$$\varepsilon'' = \varepsilon' \tan\delta \quad (2)$$

$$\sigma = 2\pi f \varepsilon_0 \varepsilon'' \quad (3)$$

Where, ε_0 = permittivity of free space, k = cell costant, ΔC = Effective capacitance, ε'' = Dielectric loss factor, σ = Dielectric coductivity values measured at limiting frequency and static frequency.

The dielectric relaxation time and the dielectric spread parameter α were evaluated using the frequency of the peak values of dielectric loss-factors for each dose and the cole-cole plots of dielectric loss factor (ε'') versus dielectric permittivity (ε') respectively. All measurement were carried out at the temperature of 28.0 ± 0.5°C and radiofrequency range of 0.5 to 50 MHz. The dielectric structure parameters were then modeled using computer aided curve fitting procedure.

RESULTS AND DISCUSSION

The dielectric conductivity (α), of the γ-irradiated bovine kidney tissue samples was found to be larger than that of the non-irradiated kidney tissue. The result also revealed that the dieletric conductivity increased with increase in gamma irradiation doses as in Table 1 and Figure 1. This

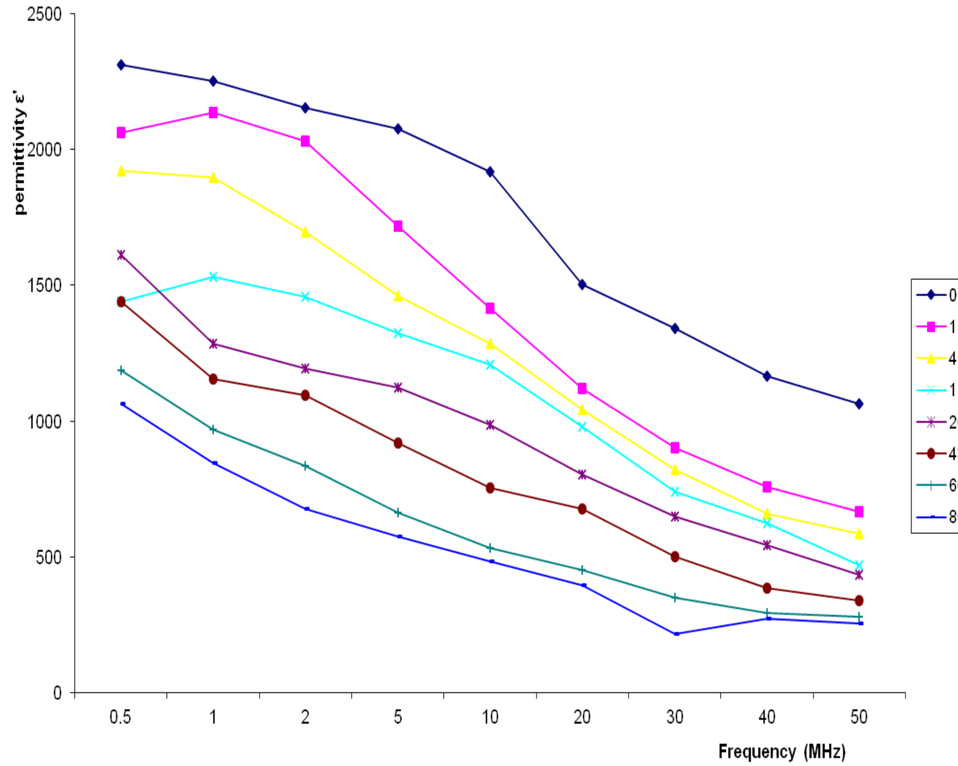

Figure 1. The mean permittivity ε' of ϒ-irradiation and non-irradiated bovin kidney from frequency range of 0.5 to 50.0 mHz.

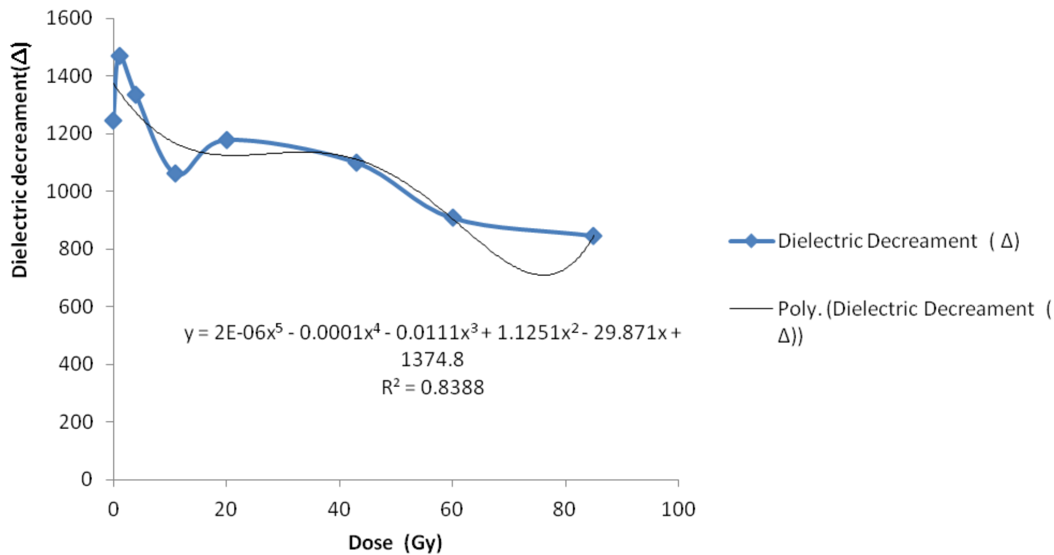

Figure 2. Variation of dielectric decrement with ϒ-irradiation dose for kidney (MHz).

may be as a result of increase in ionization produced by gamma radiation in the irradiated kidney tissues. The spread parameter (α), which isthe degree of heterogeneity in the tissue samples also increased with increase in gamma irradiation doses as shown in Figure 2 and Table 2. The curve of Figure 2 shows a sharp increase in the

Table 2. Dielectric parameter obtained from dielectric dispersion and cole-cole plots for gamma irradiation and non-irradiated bovine kidney.

Dose (Gy)	ε_s	ε_∞	$\Delta(\varepsilon_s - \varepsilon_\infty)$	τ (μs)	α
0	2311.8 ± 120	1054.6 ± 030	1247.2 ± 120	0.318 ± 0.003	0.100 ± 0.002
1	2136.9 ± 117	667.4 ± 018	1469.5 ± 117	0.318 ± 0.003	0.106 ± 0.002
4	1923.0 ± 106	586.8 ± 086	1336.2 ± 106	0.300 ± 0.001	0.104 ± 0.002
11	1531.3 ± 110	470.2 ± 066	1061.1 ± 110	0.294 ± 0.001	0.114 ± 0.004
20	1612.0 ± 124	434.1 ± 036	1177.9 ± 124	0.289 ± 0.003	0.193 ± 0.002
43	1439.6 ± 094	339.5 ± 028	1100.1 ± 094	0.276 ± 0.001	0.305 ± 0.003
60	1186.8 ± 080	278.5 ± 054	908.3 ± 080	0.274 ± 0.002	0.352 ± 0.001
85	1063.3 ± 086	217.2± 076	846.1 ± 086	0.269 ± 0.001	0.341 ± 0.005

spread parameter values from 11Gy to a peak value at 60Gy after which a gradual decrease in the spread parameter began to manifest. This indicates that the ionization produced by gamma irradiation increases the heterogeneous distribution of ions in the kidney tissues (Laogun et al., 2005).

The dieletric permittivity ε' values of γ –irradiated kidney tissues were found to decrease as the γ –irradiation doses increase as seen in Table 3 and Figure 3. Consequently, reduction in the dieletric decrement was observed as seen in Figure 4. The curve in figure 4 showed fluctuactions in dielectric permittivity value at 0Gy and a steady decrease at 20Gy – 85Gy. The decrease may be attributed to changes in the integrity and structural properties of the cellular membrane along with the reduction in the Maxwell-Wager interfacial polarization effect, which is responsible for the dielectric permittivity values at the radiofrequencies (Pettig, 1991 and Grant et al., 1978).

The dielectric relaxation time (τ), of the γ –irradiated kidney tissues decrease as the gamma irradiation doses increased as shown in Figure 5. The curve of figure 5 reveals that the relaxation time decrease steadily between 0Gy and maintained a constant value at 20Gy-43Gy after which a sharp decrease was observed between 43Gy – 85Gy. This suggest that more ions are produce in the irradiated kidney tissue. Thus, time required to charge up the cell membrane of the irradiated kidney tissue decreased.

The mathematical models developed from the dielectric parameter data obtained from experimental investigations (have about 90% fit coefficients.) are presented as:

For spread parameter, α,

(i) Bovine kidney at MHz frequency range (99.4%)

$$y = 3E - 08x^4 - 6E - 06x^3 + 0.101$$

For dielectric decrement, Δ

(ii) Bovine kidney at MHz frequency range (83.8%)

$$y = 2E - 06x^5 - 0.011x^3 + 1.125x^2 - 29.87x + 1374$$

For relaxation time

(iii) Bovine kidney at MHz frequency range (98.2%)

$$y = 2E - 08x^4 - 3E - 06x^3 - 0.004x + 0.318$$

Conclusion

The result of this investigation revealed that, γ –irradiation doses usually encountered in radiology has measurable effect on the γ –irradiated mammalian tissue and that, the extent of damage increase with increase in γ –irradiation doses. Parameters modelled suggests that, these mathematical models are adequate for generation of dielectric data which can be used in the development of dielctric imaging system for diagnosis of certain kidney disesase.

Conflict of Interests

The author(s) have not declared any conflict of interests.

ACKNOWLEDGEMENTS

We are grateful to the Director General, Nigeria Atomic Energy Commission and the Director, gamma irradiation facility, Nigeria Nuclear Technology Centre Abuja for the irradiation of our samples and in the course of this research. We are also grateful to the Technologist at the Departments of Physics and Biology of Benue State University Makurdi for their assistance throughout the period of this research.

Table 3. The mean permittivity, ε' of ϒ-irradiated and non-irradiated bovine kidney from frequency range 0.5 to 50.0 MHz.

Frequency (MHZ) / Dose (Gy)	Permittivity, ε'								
	0.5	**1.0**	**2.0**	**5.0**	**10**	**20**	**30**	**40**	**50**
0	2311.8 ± 19.6	2250.7 ± 29.6	2153.5 ± 77.8	2075.7 ± 98.2	1917.4 ±139.5	1503.5 ±105.4	1342.4 ± 74.6	1164.6 ± 54.6	1064.6 ± 96.2
1	2061.9 ± 34.2	2136.9 ± 44.6	2031.3 ± 22.6	1717.4 ± 99.2	1414.6 ± 67.8	1120.2 ± 34.7	903.5 ± 48.6	759.1 ± 27.6	667.4 ± 74.8
4	1923.0 ± 98.3	1897.8 ± 79.8	1695.2 ± 77.8	1461.8 ± 58.2	1286.9 ± 60.1	1042.4 ± 38.6	820.2 ± 64.3	659.1 ± 82.8	586.8 ± 62.6
11	1439.6 ± 98.6	1531.3 ± 78.1	1459.1 ± 49.2	1325.7 ± 90.2	1206.5 ± 54.1	978.5 ± 41.8	739.6 ± 37.3	623.0 ± 38.2	470.2 ± 63.2
20	1612.0 ± 29.3	1286.9 ± 44.9	1192.5 ± 74.1	1123.0 ± 81.2	986.8 ± 45.8	803.5 ± 85.1	648.0 ± 42.9	545.2 ± 34.6	434.1 ± 28.6
43	1439.6 ± 34.2	1156.3 ±53.0	1095.4 ± 74.8	920.2 ± 68.1	753.5 ± 68.8	678.5 ± 28.8	500.7 ± 34.8	386.8 ± 37.6	339.5 ± 77.4
60	1186.8 ± 74.3	967.4 ± 48.2	836.8 ± 51.0	661.8 ± 77.8	533.5 ± 70.1	453.5 ± 54.4	350.7 ± 59.2	292.4 ± 76.8	278.5 ± 28.9
85	1063.3 ± 124.6	846.6 ± 91.8	675.8 ± 34.6	575.8 ± 34.8	484.2 ± 66.7	396.2 ± 29.8	217.2 ± 29.4	271.6 ± 55.2	254.9 ± 47.0

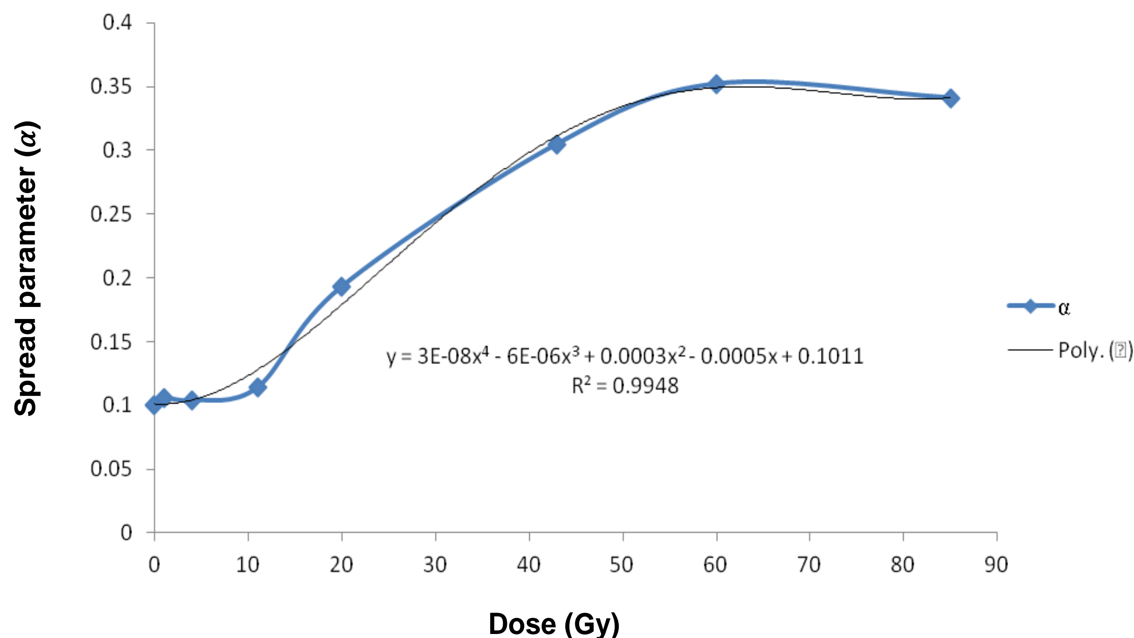

Figure 3. Variation of spread parameter With ϒ-irradiation dose for kidney (MHz).

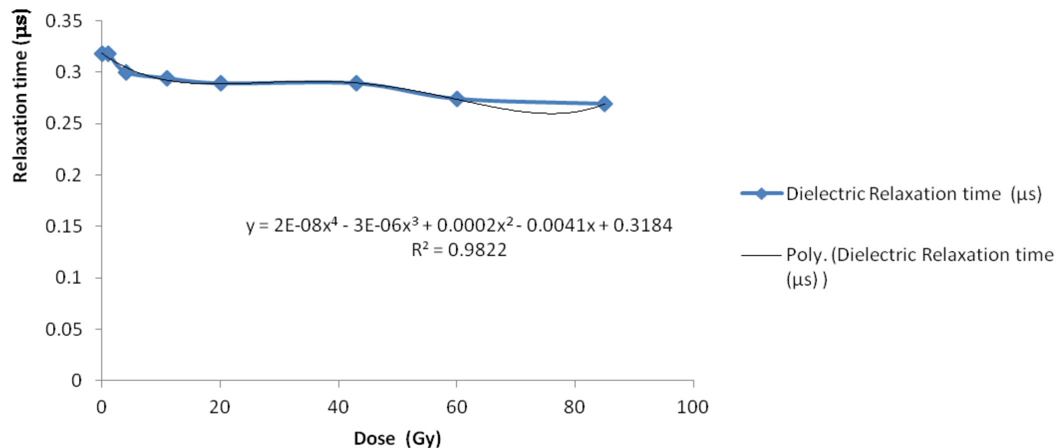

Figure 4. Variation of relaxation time with ϒ-irradiation dose for Kidney (MHz).

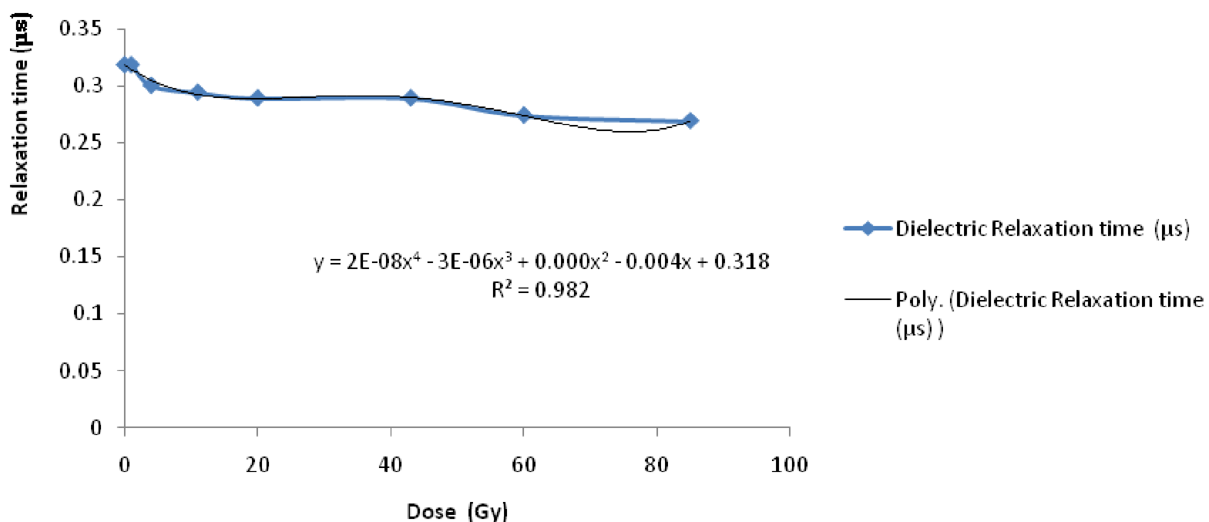

Figure 5. Variation of relaxation time with ϒ-irradiation dose for Kidney (MHz).

REFERENCES

AAMP (1992). A report of the biological effects committee of the American association of physicist in medicine published by the American institute of physics. New York, USA (3rd print).

Agba EH, Laogun AA, Ajai NO (2008). Comparism of the effect of diagnostic X-rays on the radiofrequency dielectric properties of bovine liver with bovine kidney tissues. Niger. J. Phys. 20(1):11.

Burdette EC, Fred LC, Seals J (1980). *In vivo* probe measurement techniques for determining dielectric properties of VHF through microwave frequencies IEEE Trains. Microwave theory tech. MTT-28:404-427.

Essex CG, South GP, Sheppard RJ, Grant EH (1975). A Bridge Technique for Measuring the permittivity of a Biological Solution between 1 and 100 MHZ. J. Phys. E. Scientific Instr. 8:385-389.

Grant EH, Sheppard RJ, South GP (1978). Dielectric behavior of biological molecules in solution. Clarendon Press, London.

Kyber J, Hansgen H, Pliquett F (1991). A measuring technique for the investigation of the dielectric behavior of biological tissue at low temperatures. Phys. Med. Biol. 36:1239-1243.

Laogun AA (1986). Influence of pH on the dielectric properties of egg-white lysozome in aqueous solution. J. Mol. Liq. 32:111-119.

Laogun AA, Ajayi NO, Agba EH (2005). Influence of x-rays on the radiofrequency dielectric properties of bovine kidney tissues. Niger. J. Phys. 17:117.

Pethig R (1991) Dielectric properties of tissues. In Renato Dulbecco (ed), Encyclopedia of Human Biology. Vol. 3 DI - GI, Academic Press, San Diego.

Roger C (2006). Postgraduate lecture notes on "history of radiological protection". University of Surrey, UK. (unpublished)

Russel KH, Bradley JR (2007). Intermediate physics for medicine and biology. pp. 457-463.

UNSCEAR (1993). Annex H: Radiation effects on the developing human brain.

academicJournals

Vol. 9(12), pp. 281-291, 30 June, 2014
DOI: 10.5897/IJPS2013.3838
ISSN 1992 - 1950
Article Number: 809ED7345860
Copyright © 2014
Author(s) retain the copyright of this article
http://www.academicjournals.org/IJPS

International Journal of Physical Sciences

Full Length Research Paper

Research in physical properties of $Al_xGa_{1-x}As$ III-V Arsenide ternary semiconductor alloys

Alla Srivani*, Vedam Ram Murthy and G. Veera Raghavaiah

Department of Physics, T. J. P. S College and Sri Mittapalli college of Engineering, Guntur, Andhra Pradesh, India.

Received 25 January, 2013; Accepted 28 May, 2014

General description of III-Arsenide semiconductors is presented and significance of the present work is stressed. The electrical and optical properties of III-Arsenide from binary semiconductors are evaluated using the principle of additivity involving quadratic expressions. The electrical and optical properties studied in this group include refractive index, optical polarizability, absorption coefficient and energy gap. A comparison of these data is made with reported data wherever available. The significance of the present method developed from refractive indices with out need for sophisticated experimental methods is stressed. The advantage of this group alloys is also outlined.

Key words: Physical properties, III-V group, ternary semiconductors, alliminium, gallium, arsenic.

INTRODUCTION

III-Arsenide has important position in Science and Technology of Compound semiconductors in modern electronic and optical devices. Semiconductor alloys, which are solid solutions of two or more semiconducting elements, have important technological applications, especially in the manufacture of electronic and electro-optical devices. One of the easiest ways to change artificially the electronic and optical properties of semiconductors is by forming their alloys; it is then interesting to combine two different compounds with different optical band gaps and different rigidities in order to obtain a new material with intermediate properties. Hence the major goal in materials engineering is the ability to tune the band gap independently in order to obtain the desired properties. The zinc-blende compounds AlAs, GaAs, InAs and BAs have been arousing increasing interest, both theoretically and experimentally, because of their potentially inherent advantages. There is a considerable interest in the study of ternary alloy semiconductors such as $Al_xGa_{1-x}As$, $In_xGa_{1-x}As$ with the ultimate object of providing device materials with a specific band gap and band structure. The maximum direct energy gap requirement for solar cells, light emitting diodes and semiconductor lasers has led to the use of $Al_xGa_{1-x}As$ alloys, where the band gap can be increased by addition of Al. The purpose of using Group-III Arsenide alloys is to obtain a material which consumes the minimum of power with maximum brightness. Liquid phase epitaxy compared with molecular beam epitaxy or metal organic chemical vapour deposition still continues being a useful technique for obtaining optoelectronic devices based on III–V ternary compounds. The main interest of the work is the development of the III-Arsenides for applications on current quantum well technology. In this work we report the optical and electrical characterization of $Al_xGa_{1-x}As$

*Corresponding author. E-mail: allasrivani@gmail.com
Author(s) agree that this article remain permanently open access under the terms of the Creative Commons Attribution License 4.0 International License

epitaxial layers (Puron et al., 1999).

Arsenides

We present a study of the optical and electrical properties of the AlAs, GaAs, InAs semiconductors and their alloys $Al_xGa_{1-x}As$. Because of the technological importance of $Al_xGa_{1-x}As$, its various properties have been extensively studied. In particular, parameters of the $Al_xGa_{1-x}As$ band structure have been determined from a variety of measurements, including photo response, optical transmission and photoluminescence and variation of Hall electron concentration with temperature. We present a comprehensive up-to-date compilation of band parameters for the technologically important III-V zinc blende compound semiconductors: GaAs, AlAs and InAs along with their ternary alloys. The III–V Arsenide semiconductors are important materials in the fields of fabrication of microwave, optoelectronic, and electronic devices. The film materials of devices are usually obtained by several techniques, such as metal organic vapour phase epitaxy (MOVPE), molecular beam epitaxy (MBE) and liquid phase epitaxy (LPE). Semiconductor material selection plays a vital role in developing semiconductor devices. Extensive research in materials has produced a number of compound semiconductors (Adachi, 1992).

$Al_xGa_{1-x}As$

In metal organic chemical vapour deposition (MOCVD), $Al_xGa_{1-x}As$ thin films were characterized using Raman and Hall measurements. The $Al_xGa_{1-x}As$ thin films were grown by (MOCVD using metallic arsenic instead of arsine as the arsenic precursor. Some difficulties in the growth of $Al_xGa_{1-x}As$ by MOCVD are the composition homogeneity of the layers and the oxygen and carbon incorporation during the growth process. The composition homogeneity of the films was demonstrated by the Raman measurements. Hall measurements on the samples showed highly compensated material. Samples grown at temperatures lower than 750°C were highly resistive. Independently of the V/III ratio; the samples grown at higher temperatures were n-type. As the growth temperature is increased the layers compensation decreases but the Raman spectra show that the layers become more defective (Díaz-Reyes, 2002).

METHODOLOGY

The refractive index, optical polarizability, absorption coefficient and energy gap of Arsenide semiconductor alloys are evaluated by using principle of additivity and quadratic expressions. The principle of additivity is used to study physical properties even at very small compositions. The calculated properties of refractive index, optical polarizability, absorption coefficient and energy gap versus concentrations was fitted by equations.

Table 1. Values of refractive index of binary semiconductors.

Compound	Refractive index[]n
AlAs	3.00
GaAs	3.03
InAs	3.50

Method 1

$A_{12}=A_1*x+A_2*(1-x) + 1/1000*SQRT (A_1*A_2)*x*(1-x)$

Method 2

$A_{12}=A_1*x+A_2*(1-x) +1/1000* SQRT (A_1*A_2*x*(1-x))$

Method 3

$A_{12}=A_1*x+A_2*(1-x) – 1/1000*SQRT (A_1*A_2)*x*(1-x)$

Method 4

$A_{12}=A_1*x+A_2*(1-x) – 1/1000*SQRT (A_1*A_2*x*(1-x))$

Additivity

$A_{12}=A_1*x+A_2*(1-x)$

Where A_{12} denotes refractive index (n_{12}), optical polarizability (α_{m12}), absorption coefficient (α_{12}) and energy gap (Eg_{12}). A_1 and A_2 denotes refractive index (n), optical polarizability (α_m), absorption coefficient (α), energy gap (Eg) of two binary compounds forming ternary compound.

Refractive index

The refractive index of semiconductors represents a fundamental physical parameter that characterizes their optical and electronic properties. It is a measure of the transparency of the semiconductor to incident spectral radiation. In addition, knowledge of the refractive index is essential for devices such as photonic crystals, wave guides, solar cells and detectors (Yadav et al., 2012). The refractive index values of Arsenide semiconductor alloys are evaluated by using additivity and quadratic expressions of the equations by replacing A by n the refractive index from the reported values of refractive index of binary semiconductors (Naser et al., 2009)(Table 1).

Optical polarizability

Optical polarizability (α_m) is used to study optical behaviour of binary and ternary semiconductors belonging to III-arsenide ternary semiconductor alloys.

Optical polarizability of binary compounds

Lorentz-Lorenz relation

The mean optical polarizability α_M for binary semiconductors is

obtained by using Lorentz-Lorenz relation (Sathyalatha, 2012) given below:

$$\alpha_m=\left(\frac{n^2-1}{n^2+1}\right)\frac{M}{\rho}\quad\frac{3}{4\pi N}$$

Where M, N, n, ρ refer to Molecular weight, Avogadro number, Refractive index and density

New dispersion principle

The equation of motion of the electron may be written as:

$$mZ + mbZ + \omega_0^2 mZ = eE_0 e^{i\omega t}$$

Here

$Ee^{i\omega t}$ refers to the electric force , $\omega = 2\pi\nu$, m is the electron mass, ω_0 is Natural frequency of the electron and mbZ represents the damping term.

By solving the above equation, value of z will be obtained in the form as:

$$Z=\frac{(\frac{e}{m})E_0 e^{i\omega t}}{\omega_0^2-\omega^2+i\omega b}$$

Thus the moment induced (P) per unit volume will be

P= ΣZe

$$P=\frac{\nu(\frac{e^2}{m})E_0 e^{i\omega t}}{\omega_0^2-\omega^2+i\omega b}$$

Here v is Loschmidt number. Displacement vector is obtained as:

D=E+4πp

$$D=E+4\pi\left[\frac{\nu\left(\frac{e^2}{m}\right)E_0 e^{i\omega t}}{\omega_0^2-\omega^2+i\omega b}\right]$$

$$D=E\left[1+\frac{4\pi\nu\left(\frac{e^2}{m}\right)}{\omega_0^2-\omega^2+i\omega b}\right]$$

$$\frac{D}{E}=(n-ik)^2$$

$$\frac{D}{E}=\left[1+\frac{4\pi\nu\left(\frac{e^2}{m}\right)}{\omega_0^2-\omega^2+i\omega b}\right]$$

The expression of n can be obtained by separating real and imaginary parts in the above equations that is,

$$n=1+2\pi\frac{e^2\nu}{m}\frac{\omega_0^2-\omega^2}{(\omega_0^2-\omega^2)^2+\omega^2 b^2}$$

If incident frequency $\omega<\omega_0$ then $\omega^2 b^2$ can be neglected. Thus the above equation can be written as:

$$n=1+\frac{2\pi e^2\nu}{m(\omega_0^2-\omega^2)}$$

Rearranging the terms in the above equation, we get:

$$\left[\frac{1}{\lambda_0^2}-\frac{1}{\lambda^2}\right]=\frac{e^2\nu}{2\pi c^2 m(n-1)}$$

$$\frac{1}{\lambda^2}=\alpha+\frac{\beta}{(n-1)}$$

Optical polarizability of binary compounds can be calculated by using new dispersion relation (Murthy et al., 1986) by knowing α and β values

$$\frac{1}{\lambda^2}=\alpha+\frac{\beta}{n-1}$$

Where $\alpha=\frac{1}{\lambda_0^2}$ and $\beta=-\frac{e^2\nu}{2\pi mc^2}$

Dividing through out by β and rearranging the terms n_α

$$\frac{1}{n-1}=\frac{1}{\beta\lambda^2}-\frac{\alpha}{\beta}$$

This equation is of the form Y=mx+c

$$Lt(\lambda\rightarrow\infty, \frac{1}{\beta\lambda^2}\rightarrow 0)$$

$$\text{Hence } \frac{1}{n\infty-1}=-\frac{\alpha}{\beta}=\gamma$$

$$n_\infty-1=\frac{1}{\gamma}$$

$$n_\infty=\frac{1+\gamma}{\gamma}$$

Table 2. Optical Polarizability of compounds.

Compound	Optical polarizability α_m $(cms)^3$
AlAs	71.14
GaAs	82.75
InAs	104.90

$$\frac{n_\infty^2-1}{n_\infty^2+2}=\frac{\frac{(1+\gamma)^2}{\gamma^2}-1}{\frac{(1+\gamma)^2}{\gamma^2}+2}$$

Substitute the value of $\frac{n_\infty^2-1}{n_\infty^2+2}$ in Lorentz-Lorenz formula, we get

$$\alpha_m=\left(\frac{(\gamma+1)^2-\gamma^2}{(\gamma+1)^2+2\gamma^2}\right)\frac{M}{\rho}\quad\frac{3}{4\pi N}$$

Where M, N and ρ are molecular weight, Avogadro number and density of binary semiconductors and $v=-\frac{\alpha}{\beta}$

Here α is Y-Intercept and β is the slope (Table 2).

Absorption coefficient

Lorentz-Lorenz relation for solids is represented as follows:

$$\left(\frac{n^2-1}{n^2+1}\right)=\frac{4\pi v\alpha_m}{3}$$

$$(n^2-1)=\frac{4\pi v\alpha_m.3}{3-4\pi v\alpha_m}=\left(\frac{1}{3}-\frac{1}{4\pi v\alpha_m}\right)^{-1}$$

$$\frac{1}{3}-\frac{1}{4\pi v\alpha_m}=\left(\frac{1}{n^2-1}\right)$$

$$(n^2-1)=\frac{12\pi v\alpha_m.}{3-4\pi v\alpha_m}$$

The absorption coefficient **α=2k =** $\frac{32\pi^3.}{3v\lambda^4}(n-1)^2$

From the above two equations we get

$$\frac{(n^2-1)}{(n-1)^2}=\left(\frac{12\pi v\alpha_m}{3-4\pi v\alpha_m}\right)^1\frac{32\pi^3.}{3v\lambda^4\alpha}$$

$$\frac{(n^2-1)}{(n-1)^2}=f(\text{consider})$$

$\frac{n+1}{n-1}=f$ Or $n=\frac{f+1}{f-1}$

$$n=\left(\frac{\frac{128\pi^4\alpha_m}{\alpha\lambda^4(3-4\pi v\alpha_m)}+1}{\frac{128\pi^4\alpha_m}{\alpha\lambda^4(3-4\pi v\alpha_m)}-1}\right)$$

$$\frac{n+1}{n-1}=\frac{128\pi^4\alpha_m}{\alpha\lambda^4(3-4\pi v\alpha_m)}$$

or

$$\alpha=\frac{128\pi^4\alpha_m}{\alpha\lambda^4(3-4\pi v\alpha_m)}\left(\frac{n-1.}{n+1}\right)$$

$$\alpha=\frac{128\pi^4\alpha_m}{\lambda^4}\left(\frac{n-1.}{n+1}\right)\left(\frac{M}{3M-4\pi N\rho\alpha_m}\right)$$

Here $v=\frac{N\rho}{M}$

Where N is Avogadro number ρ is the density and M is molecular weight of the semiconductor.

Thus the expression for absorption coefficient of binary semiconductor is given as (Sathyalatha, 2012):

$$\alpha=\left(\frac{128\pi^4\alpha_m}{\lambda^4}\right)\left(\frac{n-1}{n+1}\right)\left(\frac{M}{3M-4\pi N\rho\alpha_m}\right)$$

Where α_m, n, M, ρ and λ refer to the optical polarizability, refractive index, molecular weight, density and wavelength of binary semiconductors. N is Avogadro number.

Similarly for ternary semiconductors, the expression for absorption coefficient can be given as:

$$\alpha=\left(\frac{128\pi^4\alpha_{m12}}{\lambda^4}\right)\left(\frac{n_{12}-1}{n_{12}+1}\right)\left(\frac{M_{12}}{3M_{12}-4\pi N\rho_{12}\alpha_{m12}}\right)$$

Where α_{m12}, n_{12}, M_{12} and ρ_{12} are optical polarizability, refractive index, molecular weight and density of ternary semiconductor alloys and N is Avogadro number. They are calculated by using different additivity relations and quadratic expressions (Sathyalatha, 2012).

Energy gap

The electrical conductivity of semiconductors depends on width of energy gap and it is affected by Dopant composition, temperature, pressure, magnetic and electrical fields. Indirect band gap semiconductors is inefficient for emitting light. Semiconductors that have direct band gap are good light emitters. A wide band gap (WBG) semiconductor is a semiconductor with an energy band gap wider than about 2 eV, suitable for microwave devices. A narrow band semiconductor has energy band gap narrower than about 2 eV suitable for tunnel devices and infrared technology. Band gap is measured by both spectroscopic and conductivity methods.

Table 3. Energy gap of compounds.

Compound	Energy gap Eg e.v[]
AlAs	2.95
GaAs	1.42
InAs	0.36

Energy gap of ternary semiconductors

The formula used for calculation of Energy gap of ternary semiconductors are given below:

$$E_g=\left\{\frac{28.8}{((2^{x_m}-x_n)^2)^{\frac{1}{4}}}\left[\frac{1-\Phi_{12}}{1+2\Phi_{12}}\right]\right\}^{\left[\frac{x_M}{X_N}\right]^2}$$

Where x_M and x_N are the electro negativities of the constituent atoms of ternary semiconductor

$$\Phi_{12}=\left[\frac{4\pi N}{3}\right]\left[\frac{\alpha_{M_{12}}\rho_{12}}{M_{12}}\right]$$

Where $\alpha_{M_{12}}$, ρ_{12}, M_{12} and N are optical polarizability, density, molecular weight and Avogadro number of ternary semiconductor Alloys (Table 3).

RESULTS AND DISCUSSION

The refractive index values of binary Arsenide compound semiconductors are taken from reference (Naser et al., 2009) and are given in tables. The refractive index values of ternary semiconductor alloys are calculated by using different expressions of for whole composition range (0<x<1) and are presented in tables. These values are compared with literature reported data (http://www.cleanroom.byu.edu/EW_ternary.phtml-BRIGHAM; Sathyalatha, 2012). It is found that calculated values are in good agreement with reported values. Graphs are drawn for all these alloys by taking their composition values on x axis and refractive index values on y axis.

The refractive indices at various wavelengths for the binary semiconductors are taken from hand book of optical constants of solids (Edward, 1991) are presented in table along with $\frac{1}{n-1}$ and $\frac{1}{\lambda^2}$ values. The graphs drawn between $\frac{1}{n-1}$and $\frac{1}{\lambda^2}$for these semiconductors are shown in figures. From these graphs intercept α values and the slope β of the straight line are determined and γ values are calculated. All these values are given from the tables. The evaluated optical polarizabilities of binary semiconductors by using equation are also from the tables. The computed optical polarizabilities by new dispersion relations are compared with reported values.

The values of Molecular weight (M), density (ρ) and refractive index (n) of the semiconductors which are required for evaluation of α_m are taken from CRC Hand book (William and David, 2010). The energy gap values of $Al_xGa_{1-x}As$ are calculated by using different additivity expressions and presented in tables. These values are compared with Reported data (http://www.cleanroom.byu.edu/EW_ternary.phtml-BRIGHAM; Sathyalatha, 2012).

Graphs are drawn for the above $Al_xGa_{1-x}As$, alloys with variation of Dopant compositions and are given in figure. Calculated values of energy gap is taken on x axis and their composition values are taken on y axis. The refractive indices at various wavelengths for the binary semiconductors are taken from hand book of optical constants of solids (Edward, 1991) are presented in table along with $\frac{1}{n-1}$ and $\frac{1}{\lambda^2}$values.

The graphs drawn between $\frac{1}{n-1}$and $\frac{1}{\lambda^2}$ for these semiconductors are shown in figures. From these graphs intercept α values and the slope β of the straight line are determined and γ values are calculated. All these values are given from the tables. The evaluated optical polarizabilities of binary semiconductors by using equation are also from the table. The computed optical polarizabilities by new dispersion relations are compared with reported values. The values of molecular weight (M), density (ρ) and refractive index (n) of the semiconductors which are required for evaluation of α_m are taken from CRC Hand book (William and David, 2010) (Tables 4 to 11).

The applications of III-V Arsenide ternary semiconductor alloys of $Al_xGa_{1-x}As$, $In_xGa_{1-x}As$, $Al_xIn_{1-x}As$, $InP_{1-x}As_x$, $GaAs_xP_{1-x}$, $AlAs_xP_{1-x}$ as electronic, optical and optoelectronic devices are determined by elementary material properties of refractive index, optical polarizability, absorption coefficient, energy gap and mobility. Photonic crystals, wave guides and solar cells require knowledge of refractive index and energy gap of all above arsenide group alloys. The energy gap of semiconductor alloys determines threshold for absorption of photons in semiconductors. Refractive index is measure of transparency of semiconductor alloys to incident radiation. Refractive index and energy gap of ternary semiconductor alloys has significant impact on band structure. High absorption coefficient semiconductor alloys can be used for fabricating in thin film hetero junction photovoltaic (PV) devices.

Narrow band gap semiconductor alloys of $InP_{1-x}As_x$, $In_xGa_{1-x}As$ are used for photo catalytic applications. Wide band gap semiconductor alloys of $GaAs_xP_{1-x}$, $Al_xIn_{1-x}As$, $Al_xGa_{1-x}As$ are investigated for devices that allow one to

Table 4. Optical polarizability, absorption coefficient and energy Gap of $Al_xGa_{1-x}As$ X=0.09.

Wave length λ (A^0)	$\frac{1}{\lambda^2}$ In $(10)^8$ $(cms)^2$	R.I value n	$\frac{1}{n-1}$	Optical polarizability α_m $(10)^{-25}(cms)^3$		Absorption coefficient (α) $(10)^{-1}$ cms⁻	Energy gap (e.v)	
4133	5.854	4.963	0.252	Calculated	Reported Sathyalatha, 2012)	4.317	Calculated	Reported
4275	5.472	4.838	0.261	82.0	82.03	3.747	1.50	1.42
4428	5.100	4.725	0.268			3.236		
4592	4.742	4.518	0.284			2.764		
4769	4.397	4.353	0.298			2.351		
4959	4.066	4.220	0.311			1.991		
5166	3.747	4.111	0.321			1.676		
5391	3.441	4.018	0.331			1.403		
5636	3.148	3.940	0.340			1.166		
5904	2.869	3.876	0.348			0.962		
7293	1.880	3.678	0.373			0.123		
8266	1.463	3.572	0.389			0.055		

Table 5. X=0.198.

Wave length λ	$\frac{1}{\lambda^2}$ In $(10)^8$ $(cms)^2$	R.I value n	$\frac{1}{n-1}$	Optical polarizability α_m $(10)^{-25}(cms)^3$		Absorption coefficient (α) $(10)^{-1}$ cms^{-1}	Energy gap (e.v)	
4133	5.854	4.943	0.254	Calculated	Reported (Sathyalatha, 2012)	2.657	Calculated	Reported
4275	5.472	4.757	0.266	80.0	81.17	1.943	1.35	1.75
4428	5.100	4.547	0.282			1.645		
4592	4.742	4.375	0.296			1.389		
4769	4.397	4.235	0.309			1.170		
4959	4.066	4.118	0.321			0.984		
5166	3.747	4.022	0.331			0.822		
5391	3.441	3.940	0.340			0.684		
5636	3.148	3.871	0.348			0.566		
5904	2.869	3.815	0.355			0.465		
7293	1.880	3.635	0.379			0.591		
8266	1.463	3.457	0.407			0.220		
						0.193		
						0.112		

attain frequencies that span over a wide range and attain Terahertz. Applications on these ternary semiconductor alloy span from communications to biomedical engineering. Narrow band gap semiconductor alloys allow hetero junction bipolar transistors to present terahertz (THz) operation capability. Sensors of this type exploit the unique piezoelectric, polarization characteristics, as well as the high temperature stability of wide-band gap semiconductors in order to allow stable operation with high sensitivity. Using this material system one can also explore the possibility of developing fundamental sources operating in the terahertz regime

Table 6. X=0.315.

Wave length λ (A^0)	$\frac{1}{\lambda^2}$ In $(10)^8$ $(cms)^2$	R.I value n	$\frac{1}{n-1}$	Optical polarizability α_m $(10)^{-25}(cms)^3$		Absorption coefficient (α) $(10)^{-1}$ cms^{-1}	Energy Gap e.v	
4133	5.854	4.781	0.264	Calculated	Reported (Sathyalatha, 2012)	2.604	Calculated	Reported
4275	5.472	4.582	0.279	78.2	80.23	2.539	1.42	1.85
4428	5.100	4.404	0.294			2.478		
4592	4.742	4.258	0.307			2.424		
4769	4.397	4.135	0.319			2.378		
4959	4.066	4.032	0.330			2.336		
5166	3.747	3.945	0.339			2.300		
5391	3.441	3.872	0.348			2.269		
5636	3.148	3.815	0.355			2.244		
5904	2.869	3.758	0.362			2.218		
7293	1.880	3.509	0.398			2.159		
8266	1.463	3.404	0.416			2.334		

Table 7. X=0.419.

Wave length λ (A^0)	$\frac{1}{\lambda^2}$ In $(10)^8$ $(cms)^2$	R.I value n	$\frac{1}{n-1}$	Optical polarizability α_m $(10)^{-25}(cms)^3$		Absorption coefficient (α) $(10)^{-1}$ cms^{-1}	Energy Gap e.v	
4133	5.854	4.605	0.277	Calculated	Reported (Sathyalatha, 2012)	2.239	Calculate	Reported
4275	5.472	4.430	0.291	79.44	79.40	1.911	1.30	1.05
4428	5.100	4.280	0.305			1.626		
4592	4.742	4.159	0.317			1.379		
4769	4.397	4.047	0.328			1.666		
4959	4.066	4.957	0.338			0.982		
5166	3.747	3.881	0.347			0.823		
5391	3.441	3.820	0.355			0.687		
5636	3.148	3.747	0.364			0.670		
5904	2.869	3.686	0.372			0.654		
7293	1.880	3.422	0.413			0.099		
8266	1.463	3.341	0.427			0.090		

and employing micro-electro mechanical systems (MEMS) approaches.

Recent progress and new concepts using narrow and wide-band gap ternary semiconductor alloys of $Al_xGa_{1-x}As$, $In_xGa_{1-x}As$, $Al_xIn_{1-x}As$, $InP_{1-x}As_x$, $GaAs_xP_{1-x}$, $AlAs_xP_{1-x}$ and device concepts such quantum wells with very high mobility and plasma waves will lead in Terahertz detectors and emitters. Semiconductors of this type may also be used for other novel applications such as spintronics and field emission. Terahertz signal sources based on super lattices have explored applications cover a wide range of devices, circuits and components for communications, sensors and biomedical engineering.

Research on physical properties of III-Arsenide semiconductor alloys is due to operating characteristics of semiconductor devices depend critically on the

Table 8. X=0.491.

Wave length λ (A^0)	$\frac{1}{\lambda^2}$ In $(10)^8$ $(cms)^2$	R.I value n	$\frac{1}{n-1}$	Optical polarizability α_m $(10)^{-25}(cms)^3$		Absorption coefficient (α) $(10)^{-1}$ cms^{-1}	Energy Gap e.v	
4133	5.854	4.483	0.287	Calculated	Reported (Sathyalatha, 2012)	2.032	Calculated	Reported
4275	5.472	4.328	0.300	81.49	78.83	1.738	1.25	1.65
4428	5.100	4.195	0.313			1.481		
4592	4.742	4.081	0.324			1.258		
4769	4.397	3.985	0.335			1.064		
4959	4.066	3.903	0.344			0.898		
5166	3.747	3.838	0.352			0.753		
5391	3.441	3.761	0.362			0.626		
5636	3.148	3.696	0.371			0.178		
5904	2.869	3.665	0.375			0.274		
7293	1.880	3.368	0.422			0.172		
8266	1.463	3.283	0.438			0.102		

Table 9. x=0.59.

Wave length λ (A^0)	$\frac{1}{\lambda^2}$ In $(10)^8$ $(cms)^2$	R.I value n	$\frac{1}{n-1}$	Optical polarizability α_m $(10)^{-25}(cms)^3$		Absorption coefficient (α) $(10)^{-1}$ cms^{-1}	Energy Gap e.v	
4133	5.854	4.343	0.299	Calculated	Reported (Sathyalatha, 2012)	1.801	Calculated	Reported
4275	5.472	4.208	0.312	79.20	78.04	1.543	2.30	2.05
4428	5.100	4.092	0.323			1.317		
4592	4.742	3.992	0.334			1.120		
4769	4.397	3.909	0.344			0.949		
4959	4.066	3.837	0.352			0.801		
5166	3.747	3.758	0.362			0.671		
5391	3.441	3.690	0.372			0.582		
5636	3.148	3.658	0.376			0.464		
5904	2.86	3.54	0.393			0.377		
7293	1.880	3.313	0.432			0.153		
8266	1.463	3.287	0.447			0.091		

physical properties of the constituent materials. The high electron mobility of InAs, is due to its narrow band gap, makes this compound useful for very high-speed and low-power electronic and infrared optoelectronic devices.

The energy band gap of Group III-V Arsenide narrow band gap semiconductor alloys $InP_{1-x}As_x$ and $In_xGa_{1-x}As$ reduces significantly by adding a small amount of Arsenic to InP and Indium to GaAs, the band gaps of these alloys are expected to vary from 1.974 eV (InP) to 1.833 eV (InAs) in $InP_{1-x}As_x$ and 1.42 eV (GaAs) to 0.36 eV (InAs) by increasing As and In Concentrations. These ternary alloys are used for manufacturing infrared detectors, gas sensors. The energy band gaps of above two alloys decrease rapidly leading to a strong disorder when a small amount of Phosphorus atoms in InP is replaced by Arsenic and when small amount of Ga atoms are

Table 10. X=0.7.

Wave length λ (A^0)	$\frac{1}{\lambda^2}$ In $(10)^8$ $(cms)^2$	R.I value n	$\frac{1}{n-1}$	Optical polarizability α_m $(10)^{-25}(cms)^3$		Absorption coefficient (α) $(10)^{-1}$ cms^{-1}	Energy Gap e.v	
4133	5.854	4.196	0.313	Calculated	Reported (Sathyalatha, 2012)	5.873	Calculated	Reported
4275	5.472	4.084	0.324	77.96	77.16	5.042	2.50	2.36
4428	5.100	3.987	0.338			4.290		
4592	4.742	3.906	0.344			3.677		
4769	4.397	3.823	0.354			3.114		
4959	4.066	3.746	0.364			2.625		
5166	3.747	3.696	0.371			2.208		
5391	3.441	3.595	0.388			1.817		
5636	3.148	3.500	0.400			1.497		
5904	2.869	3.425	0.412			1.222		
7293	1.880	3.225	0.449			0.500		
8266	1.463	3.153	0.464			0.297		

Table 11. X=0.804.

Wave length λ (A^0)	$\frac{1}{\lambda^2}$ In $(10)^8$ $(cms)^2$	R.I value n	$\frac{1}{n-1}$	Optical polarizability α_m $(10)^{-25}(cms)^3$		Absorption coefficient (α) $(10)^{-1}$ cms^{-1}	Energy gap e.v	
4133	5.854	4.050	0.328	Calculated	Reported (Sathyalath a, 2012)	5.678	Calculated	Reported
4275	5.472	3.961	0.338	75.66	76.33	4.889	2.45	2.67
4428	5.100	3.872	0.348			4.181		
4592	4.742	3.787	0.359			3.559		
4769	4.397	3.783	0.365			3.032		
4959	4.066	3.635	0.379			2.541		
5166	3.747	3.519	0.397			2.106		
5391	3.441	3.440	0.410			1.745		
5636	3.148	3.378	0.420			1.440		
5904	2.869	3.322	0.431			0.180		

replaced by In. This occurs due to the large disparity in the electro negativity and the atomic size between P and As in $InP_{1-x}As_x$ and between In and Ga in $In_xGa_{1-x}As$. The Arsenic atom and Indium atom induces several perturbations in the host crystal (Abbasi et al., 2010).

The energy band gap of Group III-V Arsenide wide band gap semiconductor alloys $Al_xGa_{1-x}As$, $Al_xIn_{1-x}As$ and $GaAs_{1-x}P_x$ increases significantly by adding small amount of Al to GaAs, InAs and by adding As to GaP. The band gaps of these alloys are expected to vary from 1.42 eV (GaAs) to 2.67 ev (AlAs), 0.36 eV (InAs) to 2.95 eV (AlAs) and 1.42 eV (GaAs) to 2.78 eV (GaP) by increasing Al and P Concentrations. The energy band gaps of above alloys increases rapidly leading to a strong disorder when a small amount of Gallium atoms in GaAs is replaced by Al and when small amount of In atoms are replaced by Al and when small amount of As atoms are replaced by p. This occurs due to the large disparity in the electro negativity and the atomic size between Al and Ga in $Al_xGa_{1-x}As$, between Al and In in $Al_xIn_{1-x}As$ and between As and P in $GaAs_{1-x}P_x$. The Al atom and P atom induces several perturbations in the host crystal of above alloys (Djurišić, 2002).

The binding which was totally covalent for the elemental semiconductors, has an ionic component in III-V Arsenide ternary semiconductor alloys. The percentage of the ionic binding energy varies for various semiconductor alloys. The percentage of ionic binding energy is closely related to electro negativity of the elements and varies for various compounds. The electro negativity describes affinity of electrons of the element. In a binding situation the more electro negative atoms will be more strongly bind to the electrons than its partner and therefore carry net negative charge. The difference in electro negativity of the atoms in a compound semiconductor gives first measure for energy gap. A more electro negative element replacing a certain lattice atom will attract the electrons from the partner more strongly, become more negatively charged and thus increase the ionic part of the binding. This has nothing to do with its ability to donate electrons to conduction band or accept electrons from the valence band.

Mobility at high doping concentration is always decreased by scattering at the ionized dopants. Band gap increases with Electro negativity difference between the elements. Bond strength decreases with decrease of orbital overlapping. Large band gap in $Al_xGa_{1-x}As$, $Al_xIn_{1-x}As$ and $GaAs_{1-x}P_x$ is due to high degree of orbital overlapping. Electro negativity affects the width of the band gap. Electrons are more stabilized by more electro negativity atom. Pure semiconductors are located in Group 3 and 4 of the periodic table. The band gaps of these materials are less influenced by electro negativity. They are influenced by configuration of crystal lattice, valence shell electrons and hybridization of orbitals.

Semiconductor materials with higher absorption coefficients more readily absorb photons, which excite electrons into the conduction band. Knowing absorption coefficients of III-Arsenide ternary semiconductor alloys of $InP_{1-x}As_x$, $In_xGa_{1-x}As$, $Al_xGa_{1-x}As$, $Al_xIn_{1-x}As$ and $GaAs_{1-x}P_x$ aids engineers in determining which material to use in their solar cell designs. The absorption coefficient determines how far into a material light of a particular wavelength can penetrate before it is absorbed. In a material with a low absorption coefficient, light is only poorly absorbed, and if the material is thin enough, it will appear transparent to that wavelength. The absorption coefficient depends on the material and also on the wavelength of light which is being absorbed. III-V Arsenide ternary semiconductor alloys have a sharp edge in their absorption coefficient, since light which has energy below the band gap does not have sufficient energy to excite an electron into the conduction band from the valence band. Consequently this light is not absorbed.

The plot of hv versus $(\alpha hv)^2$ of III-Arsenide ternary semiconductor alloys of $InP_{1-x}As_x$, $In_xGa_{1-x}As$, $Al_xGa_{1-x}As$, $Al_xIn_{1-x}As$ and $GaAs_{1-x}P_x$ at various concentrations of As, In, Al and P forms a straight line, it can normally be inferred that there is a direct band gap, measurable by extrapolating the straight line to the α=0 axis. On the other hand, if a plot of hv versus $\alpha hv^{1/2}$ forms a straight line, it can normally be inferred that there is an indirect band gap, measurable by extrapolating the straight line to α=0 axis. Measuring the absorption coefficient for ternary semiconductor alloys gives information about the band gaps of the material. Knowledge of these band gaps is extremely important for understanding the electrical properties of a semiconductor. Measuring low values of Absorption coefficient (α) with high accuracy is photo thermal deflection spectroscopy which measures the heating of the environment which occurs when a semiconductor sample absorbs light (Priester and Grenet, 2000, 2001).

The energy levels adjust with alloy concentration, resulting in varying amount of absorption at different wavelengths in III-Arsenide ternary semiconductor alloys of $InP_{1-x}As_x$, $In_xGa_{1-x}As$, $Al_xGa_{1-x}As$, $Al_xIn_{1-x}As$ and $GaAs_{1-x}P_x$. This variation in optical properties is described by the material optical constants, commonly known as refractive index (n). The optical constants shape corresponds to the material's electronic transitions. Thus, the optical constants become a "fingerprint" for the semiconductor alloys. In $Al_xGa_{1-x}As$, the direct band gap shifts toward shorter wavelengths with increasing Al concentration. The low band gap semiconductors used in infrared detectors will absorb over most conventional ellipsometer wavelengths in $In_xGa_{1-x}As$ (Das et al., 2007).

The refractive index of Group III-V Arsenide ternary semiconductor alloys $InP_{1-x}As_x$ and $In_xGa_{1-x}As$, $Al_xGa_{1-x}As$ and $GaAs_{1-x}P_x$ reduces significantly by adding a small amount of Arsenic to InP, Indium to GaAs, Al to GaAs and P to GaAs. The refractive index of these alloys are expected to vary from 4.433(InP) to 3.157 (InAs) in $InP_{1-x}As_x$ and 4.484 (GaAs) to 4.229 (InAs) by increasing As and In concentrations. These ternary alloys are used for manufacturing infrared detectors, gas sensors. This occurs due to the large disparity in the electro negativity and the atomic size between P and As in $InP_{1-x}As_x$ and between In and Ga in $In_xGa_{1-x}As$. The Arsenic atom, Indium atom, Aluminium atom and Phosphorus atoms induces several perturbations in the host crystal.

Conflict of Interests

The author(s) have not declared any conflict of interests.

REFERENCES

Abbasi FM, Ahmad H, Perveen F, Inamullah, Sajid M, Brar DS (2010). Assesment of genomic relationship between *Oryza sativa* and *Oryza australiensis*. Afr. J. Biotechnol. 9(12):1312-1316.

Adachi S (1992). "Physical Properties of III-V Semiconductor Compounds, "John Wiley & Sons, New York.

Djurišić AB (2002). Progress in the room-temperature optical functions of semiconductors. Materials Science and Engineering R Reports 38:237.

Priester C, Grenet G (2000). “Surface roughness and alloy stability interdependence in lattice-matched and heteroepitaxy”. Phys. Rev. B. 61(23)15.

Priester C, Grenet G (2001). “Surface roughness and alloy stability interdependence in lattice-matched and heteroepitaxy”. Phys. Rev. B. 61(23)15.

Das TD, Mondal A, Dhar S (2007). IEEE International Workshop on the Physics of Semiconductor Devices (IWPSD), P. 511.

Díaz-Reyes J (2002). "Raman and Hall characterization of AlGaAs epilayers grown by MOCVD using elemental arsenic”, Superficies y Vacío15, 22-25, diciembre de ãSociedad Mexicana de Ciencia de Superficies y de Vacío.

Edward DP (1991). Handbook of Optical Constants of Solids, Volume 2, Academic press, 21 march 1991. http://www.cleanroom.byu.edu/EW_ternary.phtml-BRIGHAM YOUNG UNIVERSITY, Department of Electrical and Computer Engineering, “Direct Energy Band Gap in Ternary Semiconductors”.

Murthy VR, Jeevan kumar R, Subbaiah DV (1986). “New dispersion relation: Relation to ORD, MORD and Molecular Polarization’ Proc viii Annual conference on IEEE/EMBS, Texas, XIV, P. 1636-1639.

Naser MA, Zaliman S, Uda H, Yarub A (2009). Investigation of the absorption coefficient, refractive index, energy band gap, and film thickness for Al0.11Ga0.89N, Al0.03Ga0.97N, and GaN by optical transmission method, Int. J. Nanoelect. Mater. 2:189-195.

Puron E, Martinez-Criado G, Riech I (1999). “Growth and Optical characterization of indirect-gap AlxGa1-xAs alloys J. Appl. Phys. 86(1):1.

Sathyalatha KC (2012). PhD Thesis”Optical and related properties of few II-VI and III-V Semiconductors” SKU University, Anantapuram.

William MH, David RL (2010). CRC Hand book of Physics and chemistry, Taylor & Francis Group, 91st Edition, 26-May-2010.

Yadav DS, kumar C, Singh J Parashuram, Kumar G (2012). “Optoelectronic properties of zinc blende and wurtzite structured binary solids”. J. Eng. Comput. Innov. 3(2):26-35.

Related Journals Published by Academic Journals

- *African Journal of Pure and Applied Chemistry*
- *Journal of Internet and Information Systems*
- *Journal of Geology and Mining Research*
- *Journal of Oceanography and Marine Science*
- *Journal of Environmental Chemistry and Ecotoxicology*
- *Journal of Petroleum Technology and Alternative Fuels*

academicJournals